

**Developing an approach to study the link
between ketone bodies, K_{ATP} channels, and seizure reduction
resulting from the ketogenic diet**

Hannah Small

Honors Thesis

Submitted to:

Biology, School of Arts and Sciences

University of Richmond

Richmond, VA

April 27, 2018

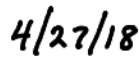
Advisor: Linda M. Boland, Ph.D.

Reader: Isaac Skromne, Ph.D.

This thesis has been accepted as part of the honors requirements in the Department of Biology.



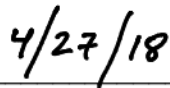
(advisor signature)



(date)



(reader signature)



(date)

Introduction

Epilepsy directly affects an estimated 65 million people globally, making it the most common, serious neurological disorder (Ngugi et al., 2010). Epilepsy encompasses many conditions but it has been loosely defined as a tendency for the brain to experience uncontrolled seizures. An epileptic seizure is defined as the symptoms of aberrant neuronal firing in the brain, which can include excessive or synchronous firing (Fisher et al., 2005). These seizures can range from a few seizures over the course of an individual's entire life to a serious epilepsy syndrome that results in hundreds of seizures a day.

The first antiepileptic drug (AED), phenobarbital, was discovered in 1912 by Alfred Hauptmann, who used it to sedate his psychiatric patients and found that it reduced their seizures (Brodie, 2010). Phenytoin was the first non-sedative antiepileptic drug, discovered in 1938 (Merritt, 1938). Since then, numerous AED's have been developed, either increasing neuronal inhibition or decreasing neuronal excitation to result in their anti-seizure effect. Many AEDs, including phenytoin, carbamazepine, lamotrigine, oxcarbazepine, and eslicarbazepine, suppress excitability by binding inactivated Na⁺ channels when the membrane is depolarized, which occurs when there is a large outward flux of K⁺ ions due to action potential firing (Yaari et al., 1986; Brodie 2010). Other broad-spectrum AEDs also bind to the sodium channel but their specific effects are unknown. Other mechanisms of AEDs include blockage of calcium channels, enhancing the response of inhibitory GABA_A receptors to GABA, altering GABA_A receptor synthesis, metabolism, or reuptake at the synapse, blockage of specific excitatory glutamate receptors, and interference with synaptic vesicle recycling (Brodie, 2010). Recently, interest has risen in potassium channel openers as targets for AEDs, specifically KCNQ2/3 and K_v1.x channels (Wickenden, 2002). Retigabine, which enhances GABAergic transmission, has been shown to open KCNQ2/3 channels, hyperpolarizing the membrane to stabilize excitability (Gunthorpe et al., 2012). However, while many epilepsies result from mutated potassium channels (Villa & Combi, 2016), there are not many drugs that act on them.

AEDs quickly gained popularity because of their ease of use and their effectiveness (Williams & Cervenka, 2017). However, an estimated 20-30% of patients with epilepsy do not respond to drugs (Picot et al., 2008; Moshé et al., 2015). The International League Against Epilepsy (ILAE) has defined drug-resistant epilepsy as a patient not achieving sustained seizure freedom after using two appropriately chosen antiepileptic drugs (Kwan et al., 2010). At this

point, the likelihood that a patient will become seizure-free with additional AEDs is less than 5% (Brodie et al, 2012). The approximately 19.5 million people that live with drug-resistant epilepsy must turn to other methods to control their seizures, including epilepsy surgery, vagus nerve stimulation or responsive neurostimulation, or lifestyle changes, like the ketogenic diet.

The ketogenic diet normally consists of a carefully maintained ratio of 3 or 4 times as many fats as combined proteins and carbohydrates, with about 90% of the total calories obtained through fat. The high-fat, low-carbohydrate diet has kept many patients seizure-free as long as they devote the necessary time and care to administer the specific nutrient ratios (Paoli et al., 2013), but it is very difficult for adults to maintain, so it is primarily used to treat epilepsy in children. For some epilepsy types, the ketogenic diet is known to effectively reduce seizures and is the standard treatment. For example, for individuals with pyruvate dehydrogenase deficiency, the ketogenic diet provides an alternative source of acetyl coenzyme A to compensate for the defective enzyme pyruvate dehydrogenase complex (Williams & Cervenka, 2017). The ketogenic diet has also been shown to be effective in reducing, and in some cases eliminating, seizures in numerous epilepsy syndromes, including Lennox-Gaustat syndrome, Dravet syndrome, Angelman syndrome, and juvenile myoclonic epilepsy (Nangia et al., 2014; Kossof et al., 2013; Thibert et al., 2012). Although the ketogenic diet is particularly effective in patients with these syndromes, it has also effectively reduced seizures in patients with symptomatic generalized epilepsy (Nei et al, 2014). An analysis of seven separate randomized, controlled trials of patients on the 4:1 ketogenic diet reported that seizure freedom has been achieved in 26% to 55% of patients and a seizure reduction of 50% or more has been observed in 38% to 85% of patients. However, patients on the ketogenic diet consistently experience negative gastrointestinal side effects, including diarrhea, constipation, and vomiting. These adverse effects were a common reason for ceasing the use of the diet (Martin et al., 2016).

While the ketogenic diet has reduced seizures in both children and adults (Schwartzkroin, 1999; Musa-Veloso et al., 2002; Williams & Cervenka, 2017), the mechanism of action remains a mystery. Since individuals who have not responded to any medications may respond to the ketogenic diet, the high fat diet may stop seizures by mechanisms different from known drugs. Establishing the mechanism of action for the anticonvulsant activity of the ketogenic diet could provide insight into a new pathway for drug development that may allow treatment with better compliance and fewer side effects.

The role of ketone bodies in the ketogenic diet

Small molecules that modulate the excitability of neurons may be important in controlling seizures. With its high fat content and low carbohydrate levels, the ketogenic diet deprives the body of the energy available from glycolysis and increases the number of fatty acids to metabolize (Masino & Rho, 2012). With an increase in the levels of fatty acids above the metabolic capacity of the tricarboxylic acid cycle, ketogenesis occurs, resulting in the production of ketone bodies, specifically acetoacetate, acetone, and β -hydroxybutyric acid (Masino & Rho, 2012). These can circulate in the blood acting as energy sources to various tissues, including the brain (Paoli et al., 2013). A leading hypothesis is that the increase in ketone bodies is the key to the mechanism of action of reducing seizures on the ketogenic diet (Schwartzkroin, 1999). This is supported by studies in rats that have found that injections of acetoacetate and acetone had anticonvulsant effects (Likhodii et al., 2003). Clinical studies have found that levels of β -hydroxybutyrate in the blood are correlated with seizure control while on the ketogenic diet (Lambrechts et al., 2016). More direct evidence has come from rodent studies where application of acetoacetate and β -hydroxybutyrate has decreased seizures in slices of substantia nigra (Ma et al., 2007). One study used knockout of BAD (BCL-2 agonist of cell death) proteins, which regulate apoptosis and glucose metabolism (Giménez-Cassina, 2012), to switch the brain's metabolic state from using glucose to using ketone bodies, mimicking the effects of the ketogenic diet. This switch resulted in a significant increase in resistance to kainic acid and pentylenetetrazole induced seizures and a reduction in the severity of the seizures in *Bad*^{-/-} mice. Interestingly, they found that the anti-seizure effect was dependent on the presence of the K_{ATP} channel by knocking out $K_{IR6.2}$, one of the subunits that make up the K_{ATP} channel, and finding that *Bad*^{-/-}*K_{IR6.2}*^{-/-} double mutant mice had a diminished seizure resistance (Giménez-Cassina et al., 2012), providing evidence that the K_{ATP} channel could be involved in the anti-seizure effects of the ketogenic diet.

K_{ATP} channels as suppressors of neuronal excitability

The K_{ATP} channel is inhibited by ATP, which makes it a unique coupler of metabolism and cellular excitability (Schwartzkroin, 1999; Yellen, 2008). In the brain, it is present in the hippocampus, cerebellum, and nuclei of the midbrain and brainstem (Karschin et al., 1997). K_{ATP} channel openers have resulted in the hyperpolarization of the membrane potentials, dampening

of cell excitability, and reduced intracellular entry of calcium (Kharade et al., 2016). In rodent hippocampal slices, perfusion of K_{ATP} channel openers cromakalim and diazoxide have suppressed hyperexcitability induced by anoxia, but did not suppress epileptiform activity induced by application of 4-Aminopyridine, a potassium channel blocker (Mattia et al., 1994), indicating the potential of K_{ATP} channels as targets for anti-epileptic drugs. However, because these channel openers are known to have effects on peripheral organs, including the pancreas, heart, and vascular system, the development of K_{ATP} channel targeting AEDs needs to be creative to differentiate between the neuronal and peripherally expressed channels (Wickenden, 2002).

Because they couple metabolism and excitability through their regulation by ATP, K_{ATP} channels are hypothesized to be involved in the mechanism of the ketogenic diet. There is some evidence in the literature linking ketone bodies and K_{ATP} channels. Genetic knockout of K_{ATP} channels in rodent substantia nigra reduced the anti-seizure effects of the ketone bodies acetoacetate and β -hydroxybutyrate (Ma et al., 2007), suggesting that K_{ATP} channels are necessary for the anticonvulsant effects of the ketogenic diet. It has been shown that application of R-BHB also increases the open probability of the K_{ATP} channel (Tanner et al., 2011). The lab that used BAD proteins to switch the state of the brain to metabolize ketones also used knockout mice to show that K_{ATP} channels are required for the anti-seizure effects. Further, they found that knockout of BAD proteins increasing the open probability of the K_{ATP} channels in mouse dentate granule neurons (Martínez-François et al., 2018; Giménez-Cassina et al., 2012). However, no study has directly tested how ketone bodies and/or ketone body metabolism regulates K_{ATP} channels to open them.

The K_{ATP} channel is modulated by pH, which may provide a link between the ketone bodies and the opening of the K_{ATP} channels. Low pH activates the K_{ATP} channel even in the presence of ATP (Wu et al., 2002). This pH sensitivity allows the channel to be regulated at physiological concentrations of ATP that normally inhibit the channel. The K_{ATP} channel has been strongly activated at pH 5.9-6.5 even in the presence of 1 mM ATP, which completely inhibits the channel at pH 7.4 (Wu et al., 2002).

There are many other hypothetical mechanisms for the seizure-reducing effects of the ketogenic diet, but my research focuses on developing an approach to study the link between these two potential players: ketone bodies and the K_{ATP} channel. I hypothesize that ketone bodies reduce excitability through pH regulation of K_{ATP} channels.

Optimization of a minimal action potential model

In order to study the role of the K_{ATP} channel in the ketogenic diet, we optimized a reduced action potential model to create an additive, controllable environment that could be used to study excitability. Dr. Carlos Villalba-Galea and Aaron Corbin introduced us to a method of exciting action potentials using the model system of *Xenopus* oocytes. I began working on optimizing this model for its use in studying excitability, specifically to study the role of K_{ATP} channels in the ketogenic diet.

Action potentials are rapid reversals of the membrane potential. Famously, Hodgkin and Huxley recorded action potentials in the giant squid axon using voltage clamp (1939). The voltage clamp methods developed by Hodgkin and Huxley also helped demonstrate that there were permeability mechanisms, or channels, involved in the action potential. These channels were distinguishable by their ion selectivities and unique kinetics, one being selective for Na^+ ions and the other being selective for K^+ ions. Both types of ions asynchronously flow down their electrochemical gradients in response to depolarization from nearby current and result in an action potential (Hodgkin & Huxley, 1952).

Voltage-gated sodium channels are integral to excitation in electrically excitable cells because they provide the explosive, regenerative inward current that initiates the rising phase of the action potential (Catterall, 2000). They are a glycoprotein complex of a pore-forming α subunit with 24 transmembrane domains and one or more auxiliary β subunits, which modulate channel gating and α -subunit plasma membrane density (Catterall, 2000; Catterall, 2005; Laedermann, 2013). To excite action potentials in oocytes we used a mouse $Na_v\alpha 1.4$ and $Na_v\beta 1.4$ channel, which is located in skeletal muscle. Co-expression of the $\beta 1$ -subunit has been shown to increase sodium channel level and hasten recovery from depolarization (Ferrera, 2006; Webb, 2008). We chose to use a skeletal muscle sodium channel because the neuronal sodium channel is notorious difficult to synthesize mRNA from. The increased current helps to evoke action potentials and the hastened recovery allows for action potentials to be excited closer to another.

Voltage-dependent potassium channels modulate the shape and frequency of action potentials, regulating excitability of neurons (Bean, 2007; Long et al., 2005). The potassium channels open after the sodium channels are activated and the outward K^+ current repolarizes the membrane. The potassium channels are made of four subunits of six transmembrane domains

and a pore loop each (Bezania, 2005). We used a *Drosophila* Kv1.1 channel with fast inactivation removed (Shaker-IR) in our oocyte model to achieve a quick membrane repolarization and to increase our chance of seeing multiple action potentials excited at one time. Shaker-IR channels mimic a delayed-rectifier channel, which helps to hyperpolarize the membrane after an action potential.

We verified the expression of the K_{ATP} channel and added it to the reduced action potential (AP) model in order to study the effects of the K_{ATP} channel on excitability in our model, with the intent on using it to investigate the link between ketone bodies and the opening of the K_{ATP} channel that has been observed previously. Integrating the K_{ATP} channel into the AP model revealed no difference in measures of excitability upon opening of the K_{ATP} channels compared to a control AP model. This may be attributable to low K_{ATP} protein levels at the membrane. Further optimization of the model is needed in order to apply it to studying the link between ketone bodies and decreasing excitability through K_{ATP} channels.

Results and Discussion

By expressing both voltage-gated potassium and sodium channels in a *Xenopus* oocyte, we can excite an action potential by using a loose voltage clamp (Figure 1; see Methods for details). The action potentials that are excited in oocytes demonstrate the typical all-or-none response, or action potential threshold of activation (Figure 1C). I also tested for the presence of a relative and absolute refractory period using two current pulses. For the relative refractory period, two current pulses of equal magnitude fail to excite a second action potential, but a small increase in the second current pulse excites an action potential (Figure 1D, left). For the absolute refractory period, no amount of current on the second pulse could excite an action potential (Figure 1D, right).

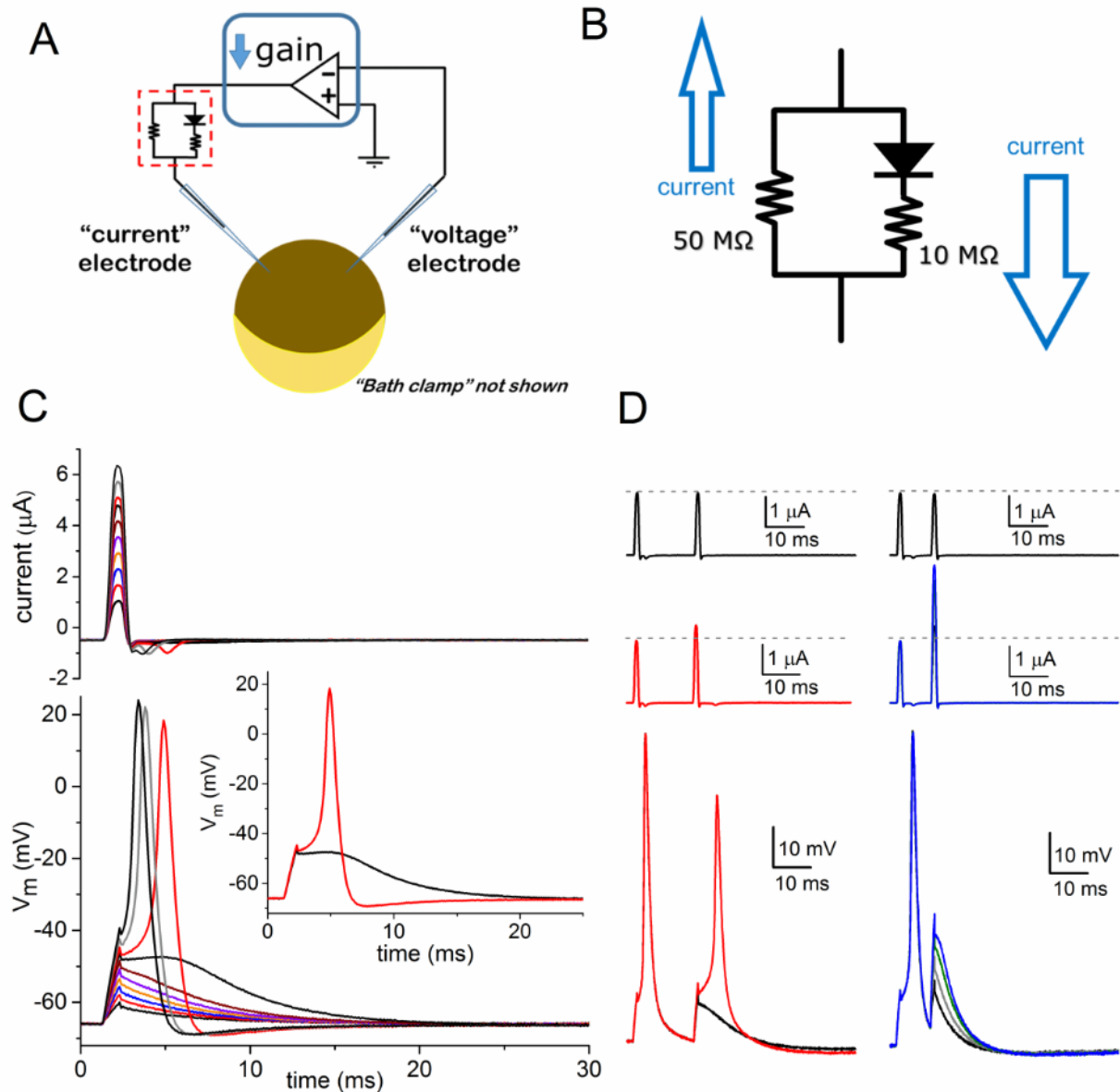


Figure 1. Action potentials recorded from *Xenopus* oocytes in loose clamp mode. (A) Schematic of the loose clamp electronics used to measure action potentials (APs) with a two-electrode voltage clamp amplifier. The dashed red box shows the adapted circuitry which is enlarged in panel B. (B) The CCHB circuit. (C) Step-wise increases in 1 ms current injections (top) were used to elicit membrane depolarizations (bottom) in oocytes injected 2 days prior with an RNA mixture for sodium and potassium channels: $\text{Na}_v1.4$ (10 ng α , 2.5 ng β), $\text{K}_v7.2$ (5 ng), $\text{K}_v7.3$ (5 ng), and Shaker-IR (0.6 ng). The inset in (C) shows a sub-threshold depolarization (black trace) and the next increase in current injection stimulated a voltage change that is an all-or-none AP (red trace). (D) Using the same RNA mixture as in panel C, the APs in oocytes were examined with two current pulses to measure the refractory period. The 1 ms current pulses (top) were 16 ms apart for the traces on the left. Two current pulses of the same amplitude (black traces) or of increasing amplitude (red traces) were used to stimulate the oocyte. The corresponding membrane voltage recordings are shown in the bottom left with the same color-coding. On the right side, the 1 ms current pulses (top) were 9 ms apart. Two current pulses of the same amplitude (black traces) or of increasing amplitude (grey, green, and blue traces) were used to stimulate the oocyte. The second stimulus was increased four times without eliciting an AP.

We also can excite multiple action potentials in an oocyte (Figure 2). Some cells have spontaneous action potential activity. This occurs frequently in cells that are injected with $K_{IR2.1}$ mRNA (Figure 2A). Typically, $K_{IR2.1}$ is used in studies to hyperpolarize the membrane and stop action potential firing (Hodge, 2009), but in our model it seems to set the resting membrane potential very close to the action potential threshold, which then induces spontaneous, rhythmic action potentials.

There are several other ways that multiple action potentials are evoked in oocytes, including multiple current pulses (Figure 2B) and a sustained, high magnitude current pulse which excites a train of action potentials (Figure 2C). These methods can be used to study the relationship between K_{ATP} and excitability.

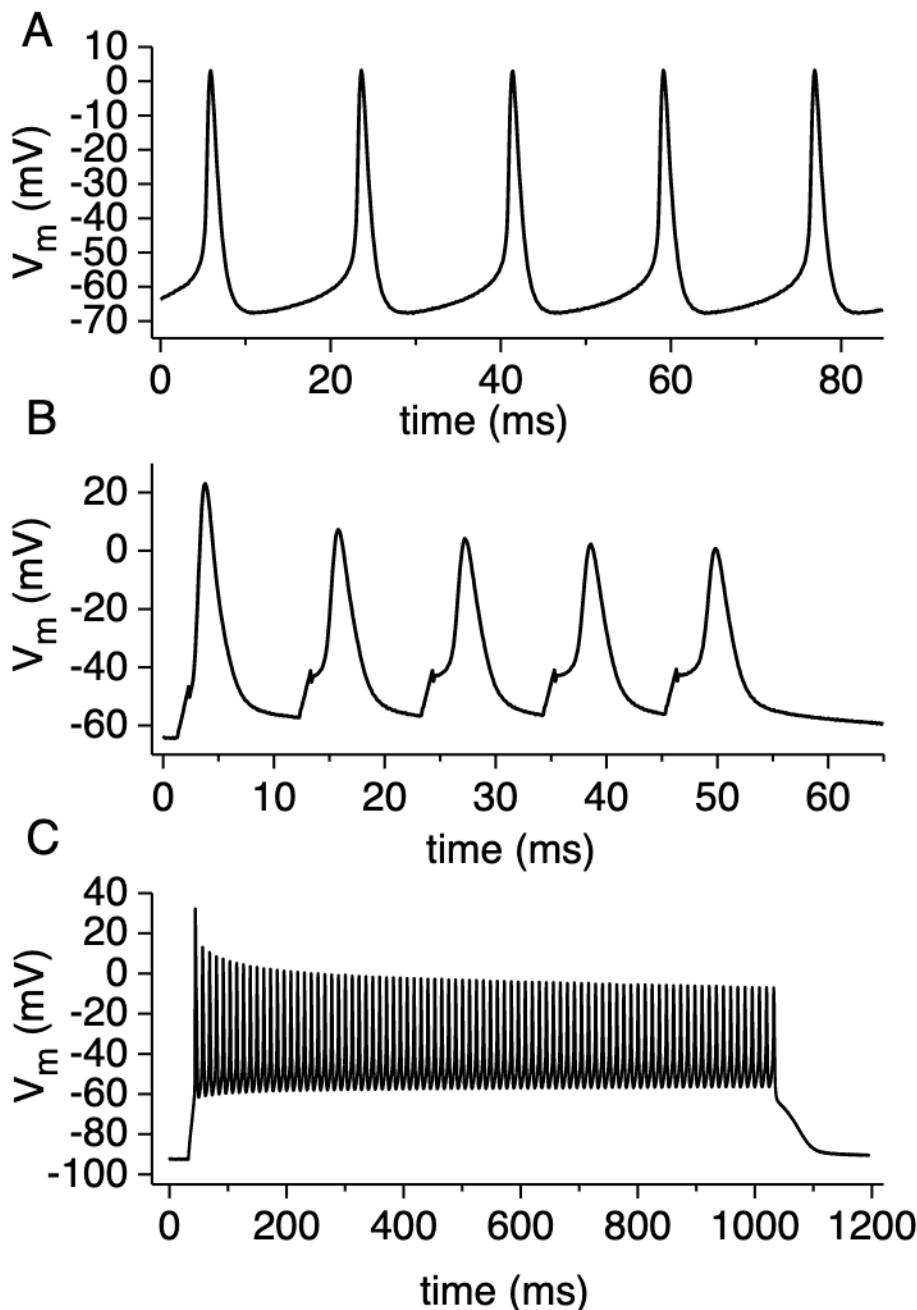


Figure 2. Oocyte recordings can demonstrate multiple APs, both induced and spontaneous. Spontaneous, unclamped action potentials (A). Oocyte was injected with 0.65 ng Shaker-IR, 10 ng $Nav1.4 \alpha$, 2.5 ng $Nav1.4 \beta$, and 10 ng $K_{IR} 2.1$ RNA and was not clamped. This is one recording from 4 similar recordings from cells injected with the same mix of RNA. (B). Oocyte was injected with 0.65 ng Shaker-IR, 10 ng $Nav1.4 \alpha$, 2.5 ng $Nav1.4 \beta$, and 10 ng $K_{IR} 2.1$ RNA and stimulus was applied from a LTEVC from -100 mV to +40 mV for 1 s. General conditions under which we observed multiple APs from multiple current stimuli (C). Multiple stimuli from a loose voltage clamp from -180 mV to +35 mV for 1 ms was applied to an oocyte injected with 0.65 ng Shaker-IR, 10 ng $Nav1.4 \alpha$, and 2.5 ng $Nav1.4 \beta$ RNA.

Integrating the K_{ATP} channel into the AP model

In order to study the K_{ATP} channel's role in the anti-seizure activity of the ketogenic diet, we need to co-express the K_{ATP} channel with a voltage-gated sodium channel and voltage-gated potassium channel. Normally, we use voltage clamp to verify the expression of both the inward sodium current and the outward potassium current, but that would not work in the case of the K_{ATP} channel because it is closed in healthy, normal conditions due to high levels of intracellular ATP. Therefore, to verify the expression of the K_{ATP} channel I had to use either a K_{ATP} channel activator, which is normally used along with application of sodium azide, an acutely toxic drug, or inhibit ATP synthesis. I decided to use FCCP (Carbonyl cyanide-p-trifluoromethoxyphenylhydrazone), an ionophore that transports protons across the mitochondrial membrane, preventing the formation of the pH gradient that normally drives ATP synthesis by ATP synthase (Benz & McLaughlin, 1983). I injected oocytes with a 1:20 ratio of h $K_{IR6.2}$ to hSUR RNA. This ratio was needed because four $K_{IR6.2}$ and four SUR1 subunits are required for the formation of a K_{ATP} channel (Craig et al., 2008), one SUR subunit per $K_{IR6.2}$ subunit (). However, the hSUR subunit is about 20x larger than the h $K_{IR6.2}$ subunit, so more mRNA must be injected to achieve 1:1 subunit interaction. Application of FCCP to these cells increased the inward current and this current was blocked by tolbutamide, a K_{ATP} channel specific blocker (Figure 3A,B). Both of these drugs were made in a solution of 100 mM K^+ , which provides a driving force for the K^+ ions to move through open channels to the inside of the cell. Cumulative data shows that the current increased 4-fold on average in K_{ATP} injected cells, while on average it did not increase the current in uninjected cells (Figure 3C). The small amount of current increase seen in some of the uninjected cells could be explained by some non-specific effects of FCCP, since it inhibits ATP synthesis, or it could be the activation of endogenous K_{ATP} channels, which are present in *Xenopus* oocytes (Pai et al., 2012). Regardless, the activation of current by inhibition of ATP synthesis and the blocking of that current with a K_{ATP} channel specific blocker in the 1:20 K_{ATP} injected cells indicates that the K_{ATP} channel is indeed being expressed in this system.

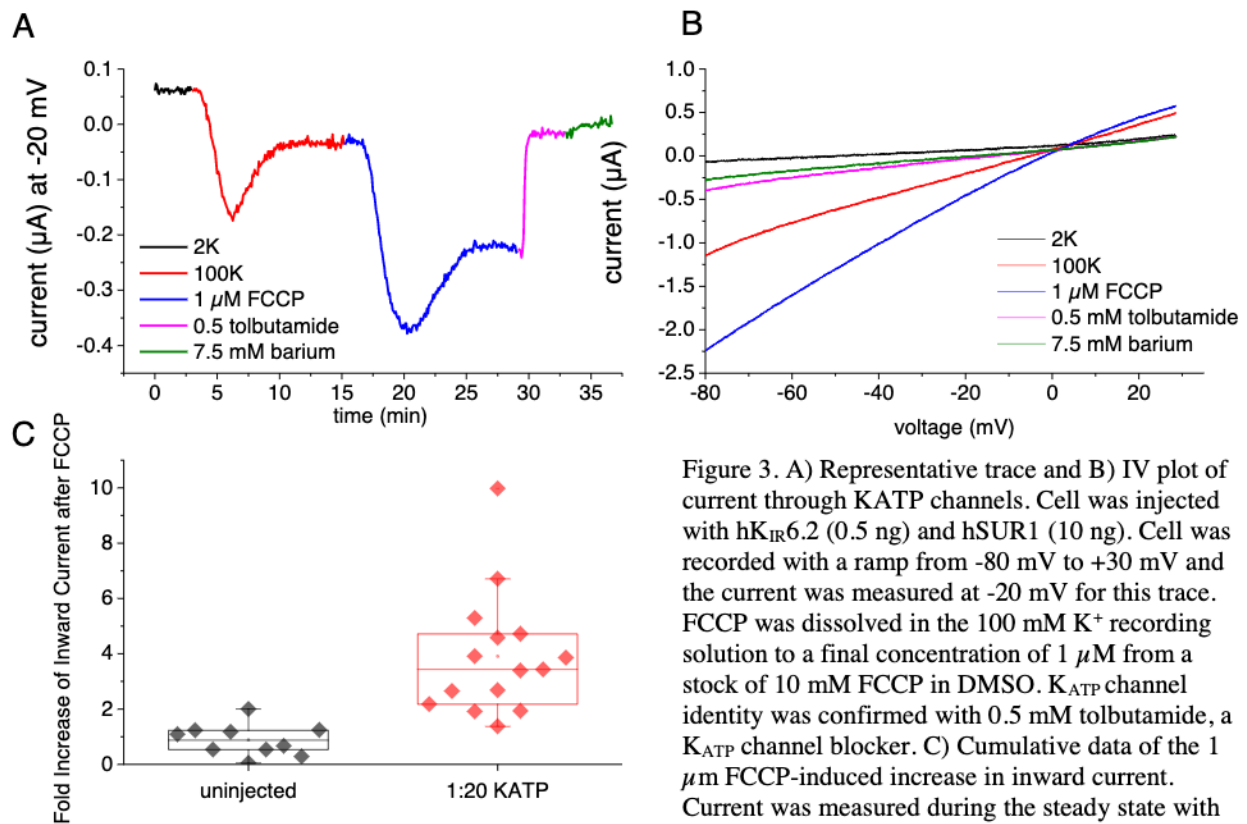


Figure 3. A) Representative trace and B) IV plot of current through KATP channels. Cell was injected with hK_{IR}6.2 (0.5 ng) and hSUR1 (10 ng). Cell was recorded with a ramp from -80 mV to +30 mV and the current was measured at -20 mV for this trace. FCCP was dissolved in the 100 mM K⁺ recording solution to a final concentration of 1 μM from a stock of 10 mM FCCP in DMSO. K_{ATP} channel identity was confirmed with 0.5 mM tolbutamide, a K_{ATP} channel blocker. C) Cumulative data of the 1 μM FCCP-induced increase in inward current. Current was measured during the steady state with perfusion with 100 mM K⁺ solution and at the maximum amount of current induced by FCCP to calculate the fold increase of inward current. One extreme outlier was left out of the 1:20 K_{ATP} injected data (a 363 fold increase). For the box plot, the whiskers represent the 25th and 75th quartile, the box indicates 50% of the data, and the line in the box represents the median.

After I established the expression of the K_{ATP} channel, I co-injected it with Nav1.4 α and β and Shaker-IR, alongside a control with just Nav1.4 α and β and Shaker-IR. I also co-injected K_{ATP} with a mix of Nav1.4 α and β , Shaker-IR, and K_{IR}2.1 to take advantage of the very excitable nature of that mix (Figure 2), but it ended up being too difficult to verify the presence of the K_{ATP} channel, since the K_{IR}2.1 channel also conducts large inward current (Figure 4). A current ramp was used to elicit the action potentials, with more and more current being injected to depolarize the cell over the sweep. This eventually results in the cell being past the threshold for Na⁺ channel activation, which stops the action potentials (Figure 4B).

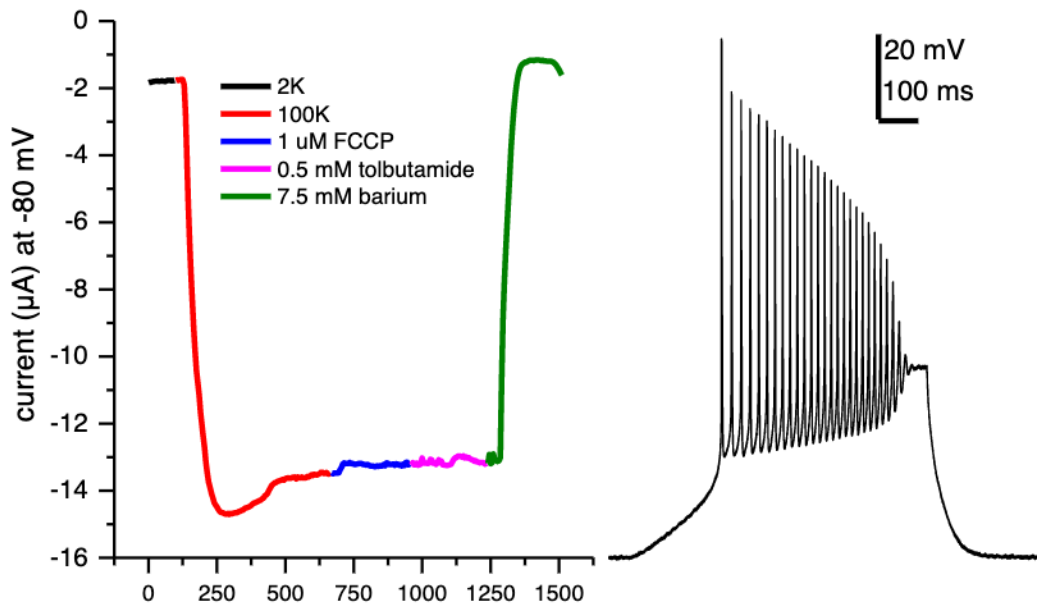


Figure 4. A) Representative trace of currents and B) representative action potential recording in an oocyte injected with $K_{IR2.1}$ (10 ng), $hK_{IR6.2}$ (0.5 ng), $hSUR1$ (10 ng), $Shaker-IR$ (0.65 ng), $Nav1.4 \alpha$ (10 ng), and $Nav1.4 \beta$ (2.5 ng).

I chose to continue working with the mix with $Nav1.4$, $Shaker-IR$, and K_{ATP} . After verifying K_{ATP} channel expression by activation upon FCCP application during voltage clamp in three cells I concluded that that batch of cells was expressing K_{ATP} and proceeded with studying the action potentials in the rest of the cells. This check was necessary because FCCP is irreversible and therefore the K_{ATP} channel expression verification via voltage clamp before studying action potentials in current clamp is not possible. In the action potential traces, there were not any obvious differences in excitability upon FCCP application between the control AP injected cells and the AP+ K_{ATP} injected cells (Figure 5).

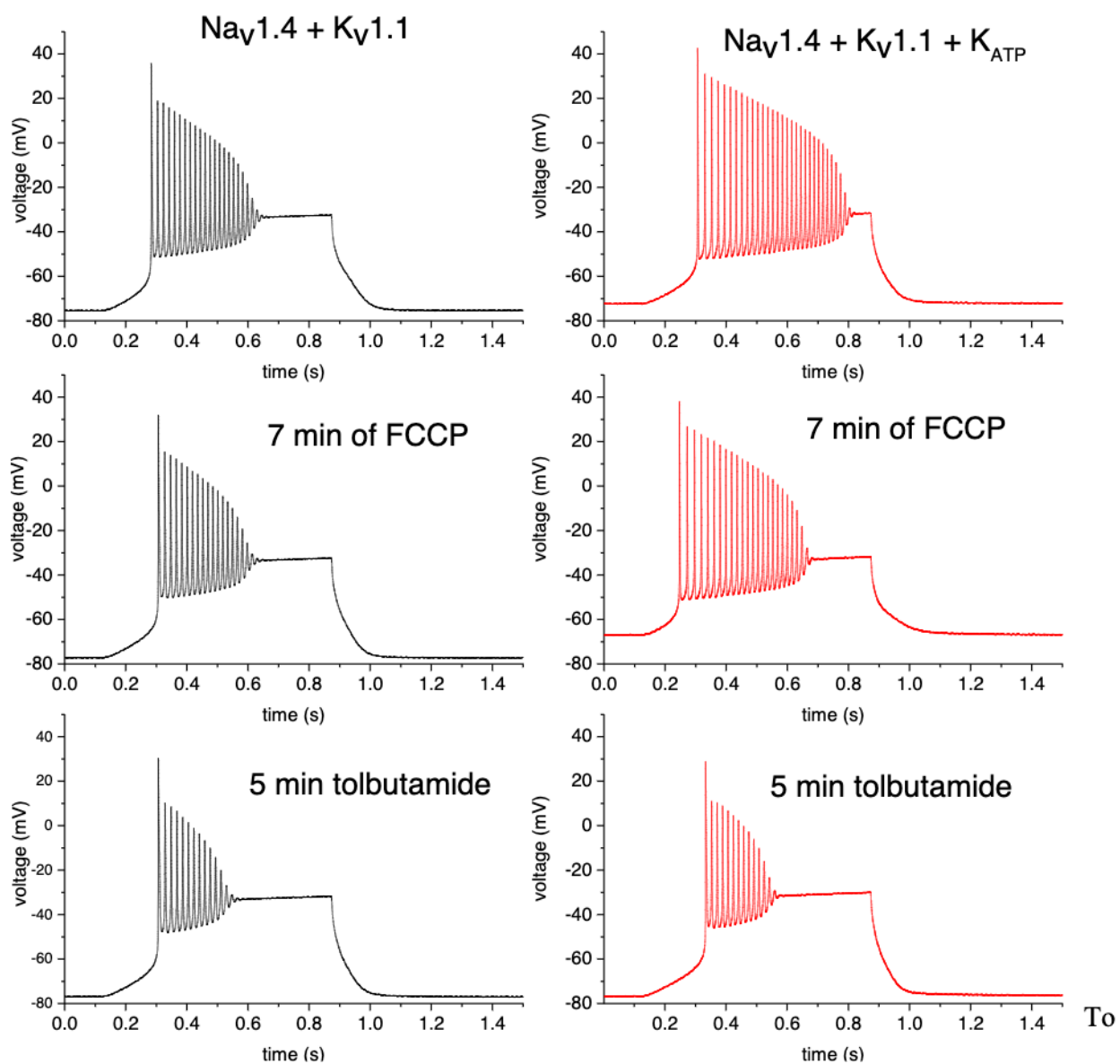


Figure 5. Traces of action potentials excited from oocytes during a recording where the oocyte was perfused with $1 \mu\text{M}$ FCCP and 0.5 mM tolbutamide. The recordings on the left were obtained from an oocyte that was injected with 2.5 ng Shaker-IR, 10 ng Nav1.4 α , and 2.5 ng Nav1.4 β . The recordings on the right were obtained from an oocyte that was injected with the same mixture with an addition of 0.5 ng of hK_{IR}6.2 and 10 ng of hSUR1.

investigate further, I analyzed several features of the action potentials excited before and after 5 minutes of FCCP perfusion and found no differences between the control and +K_{ATP} injected cells. There seem to be some differences between the states of the action potentials between the control and the AP+K_{ATP} injected cells, with the AP+K_{ATP} cells having a higher average number of action potentials and faster time to decay of the first action potential than the control cells.

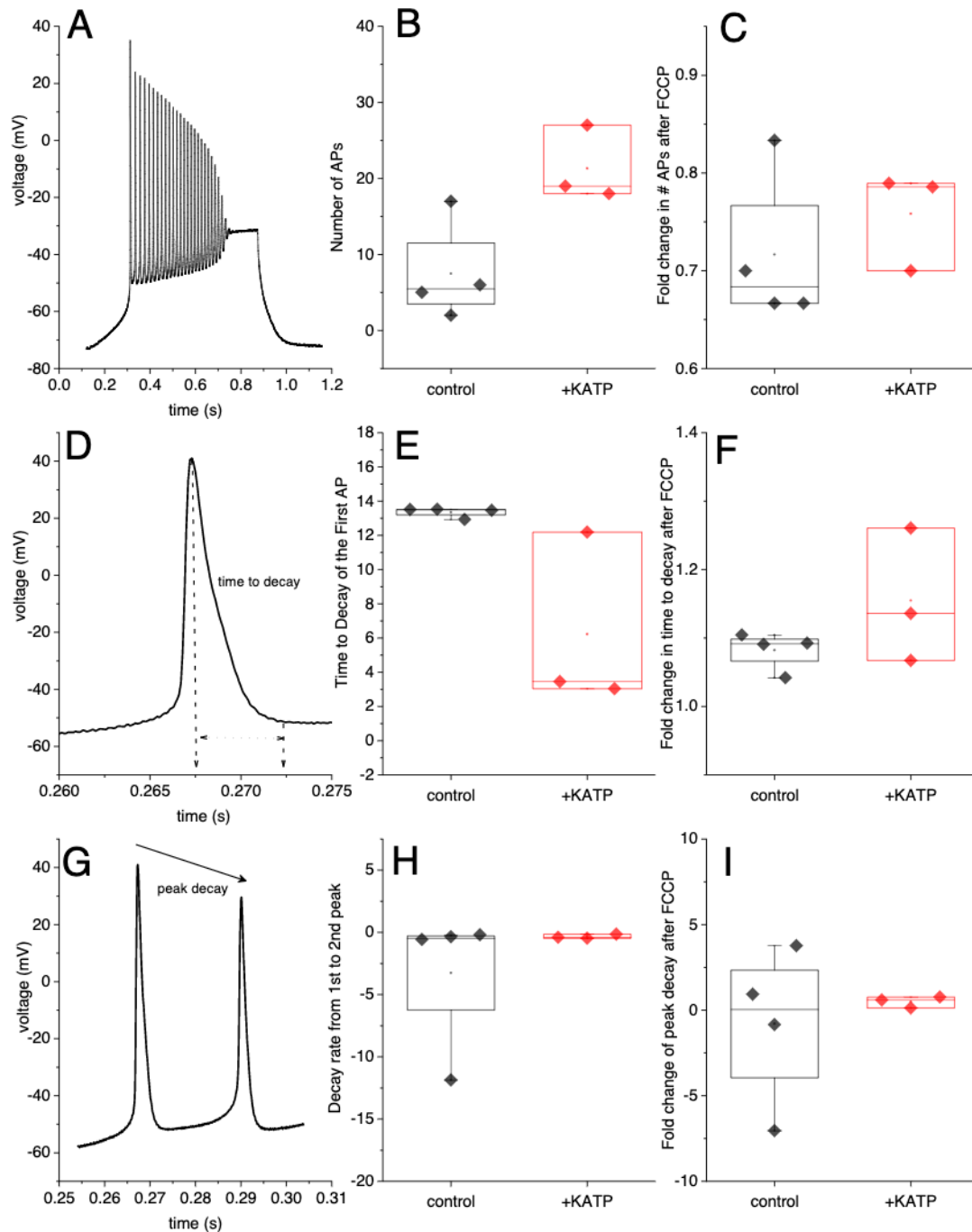


Figure 6. Analysis of action potentials after perfusion with FCCP. A) Trace recording of a cell injected with $Na_V1.4$, Shaker-IR, and K_{ATP} . B) The maximum number of action potentials during 2 mM K^+ , 98 mM Na^+ perfusion was obtained. C) The fold change of number of APs was calculated from the number of APs immediately before FCCP perfusion and after 5 minutes of 1 μ M FCCP perfusion. D) Demonstration of the time to decay feature and E) the cumulative data and F) the fold change in time to decay after 5 minutes of 1 μ M FCCP perfusion. G) Demonstration of the peak decay from the first to second AP feature and H) the cumulative data and I) the fold change in peak decay after 5 minutes of 1 μ M FCCP. For the box plots, the whiskers represent the max and min of the data, the box indicates 50% of the data, the line in the box represents the median of the data, and the dot represents the mean of the data.

These two features of the AP are related, as the faster the time to decay is, the more action potentials can be excited.

There are several reasons why the AP+K_{ATP} injected cells may display this higher AP activity: they could be expressing more Shaker-IR channels that allow faster repolarization of the membrane or the K_{ATP} channel could be imparting some sort of healthy membrane resistance that allows more action potentials to be excited. More data points need to be collected before making any conclusions about the differences between the AP and AP+K_{ATP} conditions. Even though there were some differences in the initial number of action potentials and the time to decay of the first action potential, there are no relative differences between the number of action potentials and the time to decay between AP and AP+K_{ATP} injected cells after 5 minutes of FCCP perfusion (Figure 6C, F). I also analyzed the decay rate between the amplitude of the first peak and the amplitude of the second peak generated on a particular sweep. The peak decay was very similar between the AP and AP+K_{ATP} channels with the exception of one very negative point (Figure 5H). The fold change of current after 5 minutes of 1 μ M FCCP also did not differ between the two conditions, indicating no difference in the excitability. If K_{ATP} channels are closed at rest and FCCP opens them, and the opening of K_{ATP} channels result in decreased excitability, we would expect the number of action potentials to be more reduced, the time to decay to be greater, and the peak decay to be more negative in the AP+K_{ATP} injected cells compared to the AP injected cells.

The literature has shown that the opening of K_{ATP} channels decreases excitability (Ma et al, 2007; Tanner et al., 2011; Martínez-François et al., 2018), but that is not what my data indicates. This discrepancy could exist because the K_{ATP} channels are not being opened by FCCP, but I have shown that FCCP opens K_{ATP} channels by using the K_{ATP} specific blocker in voltage clamp (Figure 3). Other explanations are that we are not measuring the right AP features to see a difference in excitability or there is low expression of K_{ATP}. I went back to the voltage clamp data to determine how much K_{ATP} current was present in the AP+K_{ATP} cells and I found that there was very little current (Figure 7A) compared to just K_{ATP} injected cells, which have an average fold increase of about 3.5 with FCCP application (Figure 3C). So, the similarity between the responses of the AP and the AP+K_{ATP} cells to FCCP may be due to low expression of K_{ATP}.

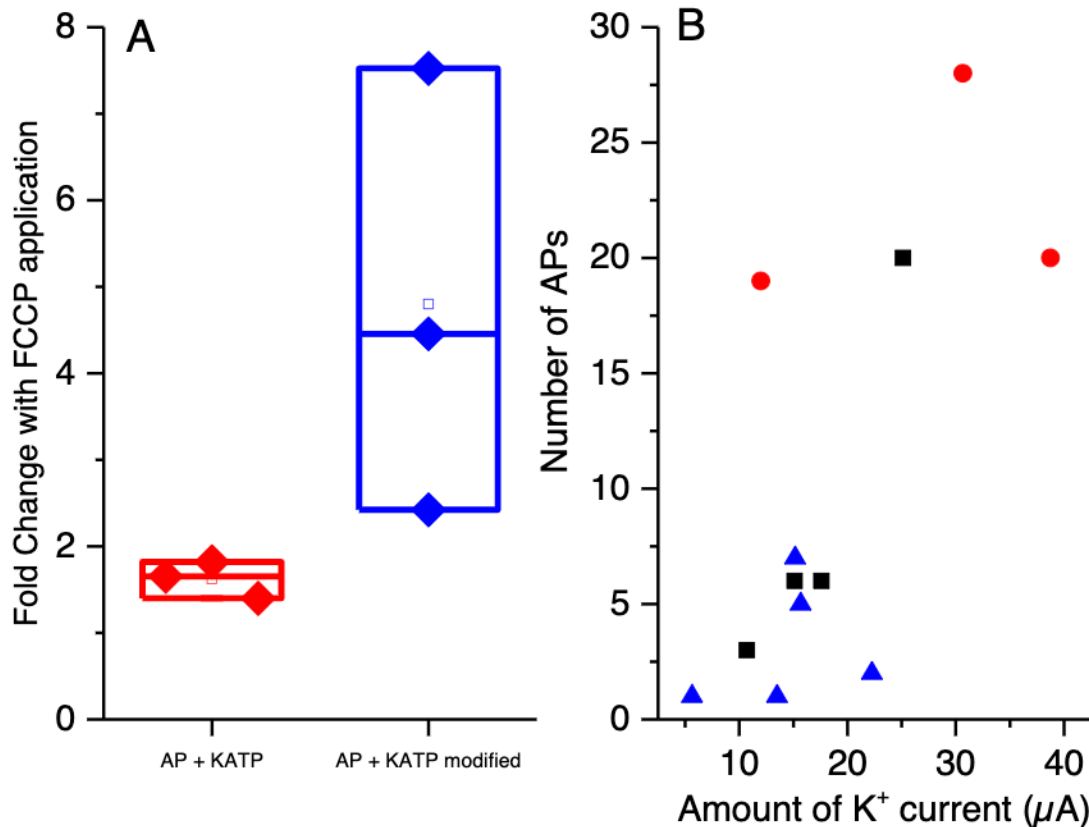


Figure 7. Optimization of the AP+K_{ATP} model. A) K_{ATP} channel expression in the AP system. The current at -60 mV before 1 μ M FCCP application and at maximal activation during 1 μ M FCCP application was measured to determine the fold change. B) The number of action potentials was counted for each cell. The amount of outward K⁺ current was measured at -10 mV with a voltage clamp. Black squares represent AP cells injected with Nav1.4 (10 ng α , 2.5 ng β) and Shaker-IR (2.5 ng). Red circles represent AP + K_{ATP} cells injected with Nav1.4 (10 ng α , 2.5 ng β), Shaker-IR (2.5 ng), hK_{IR}6.2 (0.5 ng), and hSUR1 (10 ng). Blue triangles represent AP + K_{ATP} cells injected with Nav1.4 (3.6 ng α , 0.9 ng β), Shaker-IR (0.9 ng), hK_{IR}6.2 (0.55 ng), and hSUR1 (11 ng).

The next step in the development of this model is to optimize the expression of the K_{ATP} channel in the AP model so that we can study how the regulation of the K_{ATP} channel affects the excitability. I decreased the amount of voltage-gated sodium and potassium ion channel RNA that was injected to free up cell machinery to translate, assemble, and traffic more K_{ATP} channel (referred to as AP + K_{ATP} modified). This resulted in higher expression of the K_{ATP} channel, verified through FCCP application (Figure 7A). However, the decreased expression of voltage-gated sodium and potassium ion channel RNA resulted in fewer action potentials excited in the cells (Figure 7B, blue triangles). In order to use the model for studying excitability, we need to have several action potentials, so the next immediate step is to modify the RNA mixture to get a useful balance of voltage-gated sodium and potassium channels and K_{ATP}. There is a direct positive relationship between the amount of outward potassium current and the number of APs

(Figure 7B), so we can use this relationship to create this new mixture and to resolve the differences between the AP cells and the AP + K_{ATP} cells.

One general problem with studying K_{ATP} channels is that they are closed under normal conditions due to their inhibition by ATP. This makes it difficult to verify K_{ATP} channel expression in the reduced action potential model. Currently, we are inhibiting ATP synthesis with FCCP in order to open K_{ATP} channels. This is irreversible and so cannot be studied in voltage clamp and then again in current clamp. However, this may have other non-specific health effects on the cell, which should be avoided especially while recording action potentials where a high level of membrane health should be maintained. An alternative way we could verify K_{ATP} expression would be to use K_{ATP} antibody-coated beads to identify oocytes that are expressing a certain level of K_{ATP} channels and select those to study. This could also allow the use of $K_{IR2.1}$ in the model because we would have an alternative way to check for K_{ATP} expression, although quantification of the K_{ATP} would still be difficult with $K_{IR2.1}$ present. This could expand the study to include an analysis of the K_{ATP} channels effect on spontaneous action potential activity.

After we establish the AP+ K_{ATP} model, the next phase of this research is to apply the ketone bodies to test what has been found in the literature – that the presence of ketone bodies will open the K_{ATP} channels and decrease excitability. One way this could happen is through pH regulation. The K_{ATP} channel is modulated by pH, which may provide a link between the ketone bodies and the opening of the K_{ATP} channels (Figure 8). The K_{ATP} channel has been strongly activated at pH 5.9-6.5 even in the presence of 1 mM ATP, which completely inhibits the channel at pH 7.4 (Wu et al., 2002). This pH sensitivity allows the channel to be regulated at physiological concentrations of ATP that normally inhibit the channel. There is also evidence of neuronal activity being differentially regulated by pH, therefore pH-related mechanisms could be related to the anti-excitability effects of the ketogenic diet (Masino & Rho, 2012). The metabolism of ketone bodies releases protons which could be localized in microdomains near the membrane to pH levels of 5.9-6.5, levels that activate K_{ATP} channels (Wu et al., 2002). It should be noted that FCCP could theoretically be activating the K_{ATP} channel through this mechanism, since it is a protonophore that is transporting protons into the cytoplasm. This link has not been tested.

To investigate the possible pH regulatory link between ketone body metabolism and the opening of the K_{ATP} channels, mutations can be made to the pH sensing domains of the K_{ATP}

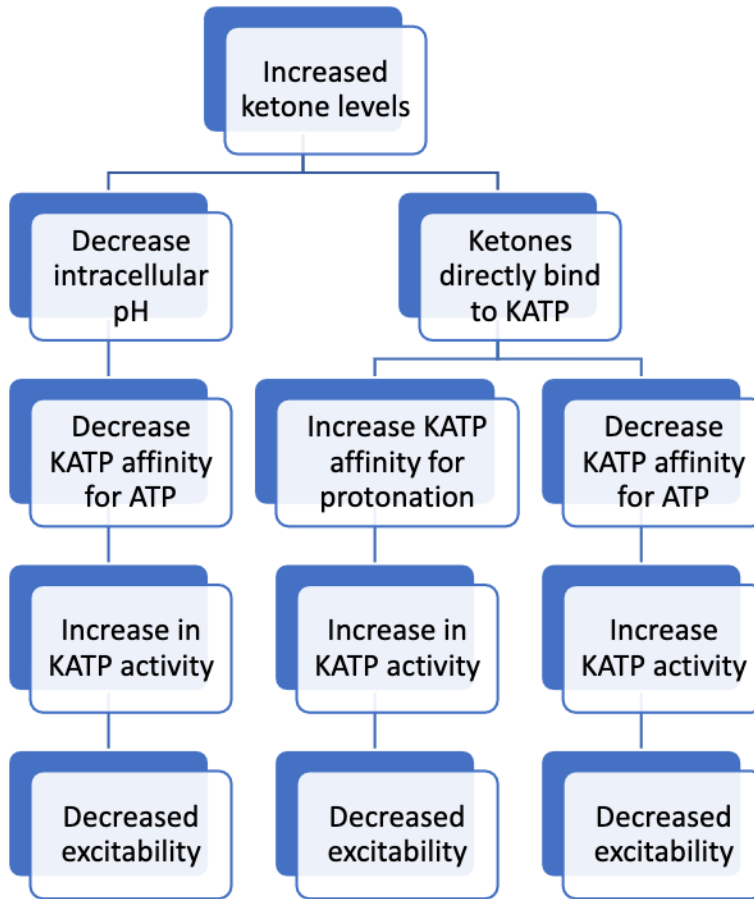


Figure 8. Hypothetical links between increased ketone levels and decreased excitability through K_{ATP} channels.

channel. Mutations made at His175 of the $K_{IR6.2}$ subunit abolishes the proton sensing (Wu et al., 2002). If pH sensing is important in the seizure suppressing effect, the excitability reduction upon ketone body application should be abolished if this His175 mutant K_{ATP} channel is expressed in the reduced AP system.

In conclusion, we have optimized a reduced action potential model that can be used to study effects of certain ion channels and their regulation of the action potential waveform and excitability. We have verified the expression of the K_{ATP} channel and are in the process of optimizing its expression in the AP model to investigate the link between ketone bodies and decreased excitability through the K_{ATP} channel. This model may be able to directly establish the relationship between ketone bodies and the opening of K_{ATP} channels. Establishing this mechanism of action could be useful in developing creative strategies for anti-epileptic drugs to target central K_{ATP} channels while leaving peripheral K_{ATP} channels unaffected.

Methods

Oocyte preparation

Processed oocytes or oocyte lobules were obtained from Ecocyte BioScience or Xenopus 1, respectively. The cells from lobules were prepared, isolated, and injected according to standard methods (Boland & Drzewiecki, 2008). The cells were isolated using 0.5 mg/ml collagenase (Collagenase 1A from Sigma/Aldrich) dissolved in a Ca^{2+} -free solution containing 96 mM NaCl, 2 mM KCl, 1 mM MgCl_2 , and 5 mM HEPES at pH 7.4. The oocytes were washed and sorted to isolate stage IV and V cells that exhibited uniform color pigmentation on the animal pole, uniform coloration of the vegetal pole, an intact membrane, and lack of a follicle cell. The RNA that was injected (see figures for mixtures and concentration information) was dissolved in DEPC water to achieve these concentrations. The injected cells were maintained at 16-18°C for two to four days in a solution of 96 mM NaCl, 2 mM KCl, 1 mM MgCl_2 , 1.8 mM CaCl_2 , 5 mM HEPES free acid, 2.5 mM Na pyruvate, 1X penicillin-streptomycin, and 5 mM sucrose.

Electrophysiology and Data Analysis

Sodium and potassium currents were recorded using standard electrophysiological methods (Boland & Drzewiecki, 2008). For the two-electrode voltage clamp (TEVC) recordings, we used an OC-725C amplifier (Warner Instruments, Hamden, CT). The voltage and current electrodes were filled with a solution of 1 M KCl, 1 mM HEPES, 10 mM EGTA, and pH 7.4. Electrodes with resistances between 0.1 and 1 M Ω were used for recordings. FCCP (BioVision) was made from a 10 mM stock in DMSO and tolbutamide (VWR) was made from a 200 mM stock in ethanol. Cells were recorded in a bath that was perfused with 2mM KCl, 98mM NaCl during the length of the recording, with the addition of indicated drugs.

A loose voltage clamp was used to record action potentials. A device that had low resistance to current flowing into the cell and high resistance to current flowing out of the cell was attached to the current electrode and the amplifier. This device inhibited the ability of the system to clamp the oocyte to a certain voltage and kept the injections of current in the oocyte's membrane instead of flowing out. The amplifier measured the membrane voltage as it responded to current injections, which excited action potentials. This device was generously made for us by Dr. Carlos A. Villalba-Galea at VCU, who introduced us to recording action potentials in oocytes.

Electrophysiological data were recorded on computers equipped with Digidata 1320A (Axon Instruments) A/D hardware. Axon's Clampex acquisition and Clampfit analysis software (versions 7-9) were used. Data were transferred over to Microsoft Excel and Microcal Origin (Northampton, MA) for analysis and production of figures.

Current ramp protocols from -150 mV to -50 mV for 750 ms were used to study multiple action potentials in AP and AP+K_{ATP} cells, with the initial resting membrane potential being set at around -80 mV using the gain. For the analysis of multiple action potentials, an action potential was defined as having a peak over -10 mV. Clampfit was used to identify these peaks and transfer the action potential data to RStudio (2016), where scripts that I wrote extracted the action potential features on each sweep. These scripts iterated through the traces to count the number of peaks on each sweep and to extract the time to decay, the peak amplitudes of the first and the second peak of each sweep to calculate the peak decay. See the R scripts for more information on this extraction.

Acknowledgements

Thanks to the Francis Ashcroft lab (Oxford) for supplying the K_{ATP} channel.

This research was funded by a Beckman Foundations Scholars Award Grant (University of Richmond), HHMI Undergraduate Science Education Program Grant (University of Richmond), and National Institutes of Health 2R15-GM096142 Grant (Linda M. Boland). Thanks to Dr. Boland for her encouragement, mentorship and guidance, Dr. Carlos Villalba-Galea and Aaron Corbin for collaborations, Trevor Larry, Jacqueline Sinnott, Bridgette Heine, Elizabeth Leggett, Shiraj Patel, Helen Robinson, and Julian Butler for assistance and discussion in the lab.

Literature Cited

- Bean BP (2007) The action potential in mammalian central neurons. *Nature Reviews Neuroscience*, 8(6): 451-465.
- Benz R, McLaughlin S (1983) The molecular mechanism of action of the proton ionophore FCCP (carbonylcyanide p-trifluoromethoxyphenylhydrazone). *Biophysical Journal*, 41(3): 381-398.
- Bezannilla F (2005) Voltage-gated ion channels. *IEEE Transactions on Nanobioscience*, 4:34-48.
- Boland LM, Drzewiecki MM (2008) Polyunsaturated Fatty Acid Modulation of Voltage-Gated Ion Channels. *Cell Biochemistry and Biophysics*, 52(2), 59-84.
- Brodie MJ (2010) Antiepileptic drug therapy the story so far. *Seizure*, 19(10): 650-655.
- Brodie MJ, Barry SJE, Bamagous GA, Norrie JD, Kwan P (2012) Patterns of treatment response in newly diagnosed epilepsy. *Neurology*, 78(20).
- Catterall WA (2000) From Ionic currents to molecular mechanisms: The structure and function of voltage-gated sodium channels. *Neuron*, 26:13-25.
- Catterall WA, Goldin AL, Waxman SG (2005) Nomenclature and structure-function relationship of voltage-gated sodium channels. *Pharmalogical Reviews*, 57: 397-409.
- Craig TJ, Ashcroft FM, Proks P (2008) How ATP inhibits the open K_{ATP} channel. *Journal of General Physiology* 132(1): 131-144.
- Ferrera L, Moran O (2006) β 1-subunit modulates the $Na_v1.4$ sodium channel by changing the surface charge. *Exp Brain Res*, 172: 139-150.
- Fisher RS, van Emde Boas W, Blume W, Elger C, Genton P, Lee P, Engel J, Jr. (2005) Epileptic Seizures and Epilepsy: Definitions Proposed by the International League Against Epilepsy (ILAE) and the International Bureau for Epilepsy (IBE). *Epilepsia*, 46(4): 470-472.
- Gunthorpe MJ, Large CH, Sankar R (2012) The mechanism of action of retigabine (ezogabine), a first-in-class K channel opener for the treatment of epilepsy. *Epilepsia*, 53(3): 412-424.
- Hodge JJ (2009) Ion channels to inactivate neurons in *Drosophila*. *Frontiers in Molecular Neuroscience*, 1.
- Hodgkin AL, Huxley AF (1939) Action Potentials Recorded from Inside a Nerve Fibre. *Nature*, 144(3651): 710-711.

- Hodgkin AL, Huxley AF (1952) The components of membrane conductance in the giant axon of Loligo. *The Journal of Physiology*, 116(4): 473-496.
- Karschin C, Ecke C, Ashcroft FM, Karschin A (1997) Overlapping distribution of K_{ATP} channel-forming $K_{IR}6.2$ subunit and the sulfonylurea receptor SUR1 in rodent brain. *FEBS Letters*, 401(1), 59-64.
- Kossof EH, Henry BJ, Cervenka MC (2013) Efficacy of dietary therapy for juvenile myoclonic epilepsy. *Epilepsy & Behavior*, 26(2): 162-164.
- Kwan P, Arzimanoglou A, Berg AT, Brodie MJ, Hauser WA, Mathern G, Moshé SL, Perucca E, Wiebe S, French J (2010) Definition of drug resistant epilepsy: Consensus proposal by the ad hoc Task Force of the ILAE Commission on Therapeutic Strategies. *Epilepsia*, 51(6): 1069-1077.
- Laedermann CJ, Syam N, Pertin M, Decosterd I, and Abriel H (2013) $\beta 1$ - and $\beta 3$ – voltage-gated sodium channel subunits modulate cell surface expression and glycosylation of $Na_v1.7$ in HEK293 cells. *Front Cell Neurosci*, 7:137.
- Lambrechts DAJE, de Kinderen RJA, Vles JSH, de Lous AJA, Aldenkamp AP, Majoie HJM (2017) A randomized controlled trial of the ketogenic diet in refractory childhood epilepsy. *Acta Neurol Scand*, 135: 231-239.
- Likhodii SS, Serbanescu I, Cortez MA, Murphy P, Snead OC, Burnham WM (2003) Anticonvulsant properties of acetone, a brain ketone elevated by the ketogenic diet. *Annals of Neurology Ann Neurol*, 54(2): 219-226.
- Long SB, Campbell EB, and MacKinnon R (2005) Crystal structure of a mammalian voltage-dependent Shaker family K^+ channel. *Science*, 309: 897-903.
- Ma W, Berg J, Yellen G (2007) Ketogenic Diet Metabolites Reduce Firing in Central Neurons by Opening K_{ATP} Channels. *Journal of Neuroscience*, 27(14): 3618-3625.
- Martínez-François JR, Fernández-Agüera MC, Nathwani N, Lahmann C, Burnham VL, Danial, NN, Yellen G (2018) BAD and K_{ATP} channels regulate neuron excitability and epileptiform activity. *ELife*, 7.
- Masino SA, Rho JM (2012) Mechanisms of Ketogenic Diet Action. *Jaspers Basic Mechanisms of the Epilepsies*, 1003-1024.

- Mattia D, Nagao T, Rogawski MA, Avoli M (1994) Potassium channel activators counteract anoxic hyperexcitability but not 4-aminopyridine-induced epileptiform activity in the rat hippocampal slice. *Neuropharmacology*, 33(12), 1515-1522.
- Merritt HH, Putnam TJ (1938) Sodium Diphenyl Hydantoinate In The Treatment Of Convulsive Disorders. *Journal of the American Medical Association*, 111(12): 1068-1073.
- Moshé SL, Perucca E, Ryvlin P, Tomson T (2015) Epilepsy: new advances. *The Lancet*, 385: 884-898.
- Musa-Veloso K, Likhodii SS, Cunnane SC (2002) Breath acetone is a reliable indicator of ketosis in adults consuming ketogenic meals. *Annals of Neurology Ann Neurol*, 54(2): 219-226.
- Nangia S, Caraballo RH, Kang H, Nordli DR, Scheffer IE (2012) Is the ketogenic diet effective in specific epilepsy syndromes? *Epilepsy Research*, 100(3), 252-257.
- Nei M, Ngo L, Sirven JI, Sperling MR (2014) Ketogenic diet in adolescents and adults with epilepsy. *Seizure*, 23(6): 439-442.
- Ngugi AK, Bottomley C, Kleinschmidt I, Sander JW, Newton CR (2010) Estimation of the burden of active and life-time epilepsy: A meta-analytic approach. *Epilepsia*, 51(5), 883-890.
- Paoli A, Rubini A, Volek JS, Grimaldi KA (2013) Beyond weight loss: a review of the therapeutic uses of very-low-carbohydrate (ketogenic) diets. *Eur J Clin Nutr*, 67(8): 789-796.
- Picot M, Baldy-Moulinier M, Dauris J, Dujols P, Crespel A (2008) The prevalence of epilepsy and pharmaco-resistant epilepsy in adults: A population-based study in a Western European country. *Epilepsia*, 49(7): 1230-1238.
- RStudio Team (2016). RStudio: Integrated Development for R. RStudio, Inc., Boston, MA URL <http://www.rstudio.com/>.
- Schwartzkroin PA (1999) Mechanisms underlying the anti-epileptic efficacy of the ketogenic diet. *Epilepsy Research*, 37(3): 171-180.
- Tanner GR, Lutas A, Martinez-Francois JR, Yellen G (2011) Single K_{ATP} channel opening in response to action potential firing in mouse dentate granule neurons. *Journal of Neuroscience*, 31(23): 8689-8696.

- Thibert RL, Pfeifer HH, Larson AM, Raby AR, Reynolds AA, Morgan AK, Thiele EA (2012) Low glycemic index treatment for seizures in Angelman syndrome. *Epilepsia*, 53(9): 1498-1502.
- Vaibhav PP, Aw S, Shomrat T, Lemire JM, Levin M (2012) Transmembrane voltage potential controls embryonic eye patterning in *Xenopus laevis*. *Development*, 139(2): 313-323.
- Villa, C., & Combi, R. (2016). Potassium Channels and Human Epileptic Phenotypes: An Updated Overview. *Frontiers in Cellular Neuroscience*, 10:81.
- Webb J, Wu F, Cannon S C (2008) Slow inactivation of the Nav1.4 sodium channel in mammalian cells is impeded by co-expression of the β 1 subunit. *Pflügers Archiv - European Journal of Physiology*, 457(6): 1253-1263.
- Wickenden, AD (2002) Potassium channels as anti-epileptic drug targets. *Neuropharmacology*, 43(7): 1055-1060.
- Williams TJ, Cervenka MC (2017) The role for ketogenic diets in epilepsy and status epilepticus in adults. *Clinical Neurophysiology*, 2: 154-160.
- Wu J, Cui N, Piao H, Wang Y, Xu H, Mao J, Jiang C (2002) Allosteric modulation of the mouse $K_{IR}6.2$ channel by intracellular H^+ and ATP. *The Journal of Physiology*, 543(2): 495-504.
- Yaari Y, Selzer ME, Pincus JH (1986) Phenytoin: Mechanisms of its anticonvulsant action. *Annals of Neurology*, 20(2): 171-184.
- Yellen, G (2008) Ketone bodies, glycolysis, and K_{ATP} channels in the mechanism of the ketogenic diet. *Epilepsia*, 49: 80-82.

Addendum

```
# AP extraction software
# Written by Hannah Small in Dr. Linda Boland's Lab
# April 2018

# Methods for extracting and plotting different features of the action
potential
# over multiple sweeps
plotCountPeaks = function(fileName, type, perfusion, sweepsOfPerfusion)
{
  # reading in the file containing the data extracted from Clampfit's
  # detect threshold feature
  APdata <- read.csv(fileName)

  #finding the maximum number of sweeps in the file
  MAX = max(APdata$Trace, na.rm = TRUE)
  show(MAX)

  #initialize all to 0
  traceExtraction = rep(0, MAX)

  i = 1

  #iterating through the traces in the file to extract the number of peaks
  while(i < length(APdata$Trace))
  {
    temp = APdata$Trace[i]

    j = i + 1
    count = 1

    #this loop counts the number of peaks on a certain trace
    while(temp == APdata$Trace[j] && j <= length(APdata$Trace)){
      j = j + 1
      # add to the current number of peaks
      count = count + 1
    }
    traceExtraction[temp] = count

    #reset the iterator
    i = j
  }

  #plotting the number of peaks vs. the traces to see the # of peaks over the
  #time of the recording
  graphTitle = paste(type, fileName, sep = ", ")

  plot(x = 1:MAX, y = traceExtraction, xlab = "trace", ylab = "Number of
  APs", main = graphTitle)

  addPerfusionInfo(perfusion, sweepsOfPerfusion, max(traceExtraction))

  return(traceExtraction)
}
```

```

plotTimeToDecayOfFirst = function(fileName, type, perfusion,
sweepsOfPerfusion, y)
  APdata <- read.csv(fileName)

  MAX = max(APdata$Trace, na.rm = TRUE)

  #initialize all to 0
  traceExtraction = rep(0, MAX)

  trace = 1 #starting trace
  for(i in 1:nrow(APdata)){
    if(trace == APdata$Trace[i])
    {
      traceExtraction[trace] = APdata$TimeToDecay[i+1] #use i+n to get data
for the second, third, etc peak
      trace = trace + 1
    }
  }

  graphTitle = paste(type, fileName, sep = ", ")

  plot(x = 1:MAX, y = traceExtraction, xlab = "trace", ylab = "Time to Decay
of first AP (ms)", main = graphTitle, ylim = c(11, 14))

  addPerfusionInfo(perfusion, sweepsOfPerfusion, max(traceExtraction))

  return (traceExtraction)
}
#used to obtain data to calculate the peak decay
plotFirstPeak = function(fileName, type, perfusion, sweepsOfPerfusion,y =
90){
  APdata <- read.csv(fileName)

  MAX = max(APdata$Trace, na.rm = TRUE)

  #initialize all to 0
  traceExtraction = rep(0, MAX)

  trace = 1 #starting trace
  for(i in 1:nrow(APdata)){
    if(trace == APdata$Trace[i])
    {
      #get first AP and add the baseline
      traceExtraction[trace] = APdata$PeakAmp[i] + APdata$Baseline[i]
    }
  }

  graphTitle = paste(type, fileName, sep = ", ")

  plot(x = 1:MAX, y = traceExtraction, xlab = "trace", ylab = "Peak amplitude
of first AP (mV)", main = graphTitle)

  addPerfusionInfo(perfusion, sweepsOfPerfusion, max(traceExtraction))

  return(traceExtraction)
}

```

```

#used to obtain data to calculate the peak decay
plotSecondPeak = function(fileName, type, perfusion, sweepsOfPerfusion, y)
#could add in the perfusion solutions later
{
  APdata <- read.csv(fileName)

  MAX = max(APdata$Trace, na.rm = TRUE)

  #initialize all to 0
  traceExtraction = rep(0, MAX)

  trace = 1 #starting trace
  for(i in 1:nrow(APdata)){
    if(trace == APdata$Trace[i])
    {
      #get second AP - if you want second or more AP, change i to i + n
      traceExtraction[trace] = APdata$PeakAmp[i + 1] + APdata$Baseline[i +
1]#get second AP - if you want second or more AP, change i to i+ n
      trace = trace + 1
    }
  }

  graphTitle = paste(type, fileName, sep = ", ")

  plot(x = 1:MAX, y = traceExtraction, xlab = "trace", ylab = "Peak amplitude
of second AP (mV)", main = graphTitle)

  addPerfusionInfo(perfusion, sweepsOfPerfusion, max(traceExtraction))

  return(traceExtraction)
}

#timeOfPerfusion must always have one more entry than perfusionID (the ending
sweep)
#method for plotting the perfusion information on the graph
addPerfusionInfo = function(perfusionID, timeOfPerfusion, y)
{
  # show(n(perfusionID))
  for (i in 1:length(perfusionID))
  {
    text(x = timeOfPerfusion[i] + 50, y = 2, labels = perfusionID[i], cex =
0.5)
    arrows(x0 = timeOfPerfusion[i], y0 = 3, x1 = timeOfPerfusion[i+1], y1 =
3, angle = 90)
  }
}

```

Example entry of perfusion data to make a plot:

```

perfusion <- c("2K", "1 uM FCCP in 2K", "0.5 mM tolbutamide in 2K", "2K", "0.5
tolbutamide in 2K", "2K", "1 uM FCCP in 2K")
sweepsOfPerfusion <- c(0, 34, 442, 500, 645, 735, 900, 942)

```

Example use of a method:

```
perfusion <- c("2K", "1 uM FCCP", "2K", "1 uM FCCP", "2K")
sweepsOfPerfusion <- c(0, 225, 429, 670, 965, 1145)

plotFirstPeak("2018_02_09_0026.csv", "AP15", perfusion, sweepsOfPerfusion)
plotSecondPeak("2018_02_09_0026.csv", "AP15", perfusion, sweepsOfPerfusion)
```